Conformational Studies of Methyl 3-*O*-Methyl-α-D-arabinofuranoside: An Approach for Studying the Conformation of Furanose Rings

Justin B. Houseknecht, Patrick R. McCarren, Todd L. Lowary,* and Christopher M. Hadad*

Contribution from the Department of Chemistry, The Ohio State University, 100 West 18th Avenue, Columbus, Ohio 43210

Received October 24, 2000. Revised Manuscript Received July 2, 2001

Abstract: A computational method for probing furanose conformation has been developed using a methylated monosaccharide derivative **1**. First, a large library of conformers was generated by a systematic pseudo Monte Carlo search followed by optimization with the AMBER molecular mechanics force field. A subset of these conformers was then subjected to ab initio and density functional theory calculations in both the gas and aqueous phases. These calculations indicate that entropic contributions to the Gibbs free energy are important determinants of the Boltzmann distribution for the conformational preferences of **1** in the gas phase. The results obtained at each level of theory are discussed and compared with the experimentally determined conformer distribution from NMR studies in aqueous solution. In addition, the ability of each level of theory to reproduce the experimentally measured $^1H-^1H$ coupling constants in **1** is discussed. Empirical Karplus equations and density functional theory methods were used to determine average $^3J_{H1,H2}$, $^3J_{H2,H3}$, and $^3J_{H3,H4}$ for each level of theory. On the basis of this comparison, consideration of solvation with the MN-GSM model provided good agreement with the experimental data.

Introduction

The determination of macromolecular structure is a subject of increasing importance. X-ray crystallography and NMR spectroscopy have been used to determine the three-dimensional structure of nucleic acids[1a] and proteins,[1b] and recent progress in the field of carbohydrate chemistry has provided an understanding of the three-dimensional structure of oligosaccharides containing pyranose residues.[1c] In contrast, the conformational preferences of oligosaccharides composed of furanose moieties are not well understood. This is due both to a lack of experimental data on oligofuranosides and the significant flexibility of five-membered rings. A greater understanding of the conformational preferences of oligofuranosides is, however, desirable because of the important role that these glycans play in many bacterial infections, in particular those arising from mycobacteria.[2]

The solution conformation of a furanose ring is generally described by a model in which two local minimums interconvert via pseudorotation.[3a] This model makes use of the pseudorotational wheel (Figure 1). One minimum generally lies in the northern hemisphere (the N conformer); the other minimum occurs in the southern hemisphere (the S conformer). For D-aldofuranoses, pseudorotation occurs through the east rather than the west[3b] because the latter pathway proceeds through conformers in which the hydroxymethyl group at C_4 is pseudoaxial. Conformer equilibration through the planar form is generally unfavorable due to the necessary eclipsing of all ring substituents in this structure.

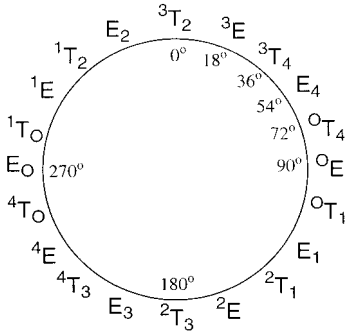

Figure 1. Pseudorotational wheel for a D-aldofuranose.

Initial experimental studies[4] of furanose conformational preferences were pursued for the D-ribofuranosyl and 2-deoxy-D-*erythro*-pentofuranosyl units of RNA and DNA, respectively. A detailed understanding of the conformational behavior of these ring systems in nucleic acids is now available,[5,6] and an increasing number of experimental investigations have focused

(1) (a) Mollova, E. T.; Pardi, A. *Curr. Opin. Struct. Biol.* **2000**, *10*, 298. (b) Powell, H. R. *Annu. Rep. Prog. Chem., Sect. C: Phys. Chem.* **2000**, *96*, 139. (c) Jimenez-Barbero, J.; Asensio, J. L.; Canada, F. J.; Poveda, A. *Curr. Opin. Struct. Biol*. **1999**, *9*, 549.

(2) Brennan, P. J.; Nikaido, H. *Annu. Rev. Biochem.* **1995**, *64*, 29.

(3) (a) Altona, C.; Sundaralingam, M. *J. Am. Chem. Soc.* **1972**, *94*, 8205. (b) Harvey, S. C.; Prabhakaran, M. *J. Am. Chem. Soc.* **1986**, *108*, 6128.

(4) Sundaralingam, M. *J. Am. Chem. Soc.* **1965**, *87*, 599.

(5) (a) Saenger, W. *Principles of Nucleic Acid Structure*; Springer-Verlag: Berlin, 1988. (b) Birnbaum, G. I.; Shugar, D. Biologically Active Nucleosides and Nucleotides: Conformational Features and Interaction with Enzymes. In *Topics In Nucleic Acid Structure*; Neidle, S., Ed.; MacMillan Press: London, 1987; p 1.

(6) (a) Bandyopadhyay, T.; Wu, J.; Stripe, W. A.; Carmichael, I.; Serianni, A. S. *J. Am. Chem. Soc.* **1997**, *119*, 1737. (b) Church, T. J.; Carmichael. I.; Serianni, A. S. *J. Am. Chem. Soc.* **1997**, *119*, 8946. (c) Bandyopadhyay, T.; Wu, J.; Serianni, A. S. *J. Org. Chem.* **1993**, *58*, 5513. (d) Kline, P. C.; Serianni, A. S. *J. Org. Chem.* **1992**, *57*, 1772. (e) Podlasek, C. A.; Stripe. W. A.; Carmichael, I.; Shang, M.; Basu, B.; Serianni, A. S. *J. Am. Chem. Soc.* **1996**, *118*, 1413.

10.1021/ja003768s CCC: $20.00
Published on Web 08/11/2001

on other biologically important furanose moieties. These studies have been carried out on monosaccharides[7] as well as oligosaccharides.[8]

Computational methods have also been used to study the conformational preferences of furanosides. The majority of these investigations have involved molecular mechanics calculations.[8b,j,k,9] However, studies using ab initio and density functional theory (DFT) methods have also been reported.[6a,b,7f,10]

With the exception of the furanose residues present in nucleic acids, no molecular mechanics force field has been explicitly parametrized for furanose rings.[11] However, results in good agreement with experiment have been obtained for other furanose derivatives with a number of the standard force fields (e.g., AMBER and more often MM2 and MM3).[8j,k,9] For monosaccharides, much of the work has focused on building thousands to millions of conformers through variations of ring puckering and torsion angles about endocyclic and exocyclic bonds and subsequent minimization (the flexible residue method).[9a−f] However, in some cases, conformational searching methods have been used.[9i] For oligosaccharides, initial geometries for molecular mechanics calculations have usually been obtained by combination of the known low-energy conformers of the constituent monosaccharides or by using available crystal structures.[8b,j,k,9f,g,k−n] Dihedral driving techniques have then been used to explore the conformational space about the glycosidic bonds. A less common approach is the generation of starting geometries by random Monte Carlo searches.[9g,h,o]

Given the limitation of computational resources, ab initio and DFT calculations of furanose rings have necessarily involved a subset of all possible conformers to produce a partial potential energy surface. This has typically been done by considering only the idealized envelope geometries and a limited number of the possible rotamers around exocyclic bonds.[10a,b,f,g] However, recent studies on D-fructofuranose[10e] and methyl α-D-lyxofuranoside[10i] have probed both twist and envelope conformers. In these studies, intuition was used to select the conformers that were investigated. In such investigations, particular attention must be paid to torsion angles about exocyclic bonds when the conformers are chosen. In some cases, this choice is straightforward; for example, the torsion angle about the C_1-O_1 bond is generally fixed in the orientation preferred by the exoanomeric effect. However, often the bond rotamers that should be investigated are less clear. For example, it is often difficult to determine what staggered orientation about a given exocyclic OH bond should be used. This is an important issue because the barrier to rotation about these bonds is generally significant, and consequently, these conformers may reside in local minimums that are different from the true global minimum. Unfortunately, given the paucity of X-ray and NMR data for furanosides, experimental studies cannot always be used as a basis for deciding which conformers to investigate. Clearly, with larger systems, including oligosaccharides containing furanose residues, a more efficient method must be used. In these larger molecules, the number of possible conformers becomes enormous and intuition is a less reliable guide. One obvious approach is to use molecular mechanics searching algorithms to generate and minimize a large number of conformers and then study a portion of these at higher levels of theory. Although this approach has been applied to pyranosides,[12] it has found limited application with furanose rings.[9i,j,o,10c]

In this report, we describe a method for assessing the conformational preferences of furanose rings that couples a molecular mechanics conformational search with high-level ab initio and DFT calculations. First, a systematic pseudo Monte Carlo (SPMC)[14b] search is used to generate a large number of conformers that are minimized using the AMBER* force field.[13] Subsets of the resulting conformers are then subjected to further ab initio and DFT optimizations in both the gas phase and in

(7) (a) Wu, G. D.; Serianni, A. S.; Barker, R. *J. Org. Chem.* **1983**, *48*, 1750. (b) Serianni, A. S.; Barker, R. *J. Org. Chem.* **1984**, *49*, 3292. (c) Moravcová, J.; Capková, J.; Stanek, J.; Raich, I. *J. Carbohydr. Chem.* **1997**, *16*, 1061. (d) Rubira, M.-J.; Jimeno, M.-L.; Balzarini, J.; Camarasa, M.-J.; Pérez-Pérez, M.-J. *Tetrahedron* **1998**, *54*, 8223. (e) Serianni, A. S.; Wu. J. Carmichael, I. *J. Am. Chem. Soc.* **1995**, *117*, 8645. (f) O'Leary, D. J.; Kishi, Y. *J. Org. Chem.* **1994**, *59*, 6629. (g) Varela, O.; Marino, C.; Cicero, D. *An. Asoc. Quim. Argent.* **1992**, *79*, 107. (h) Angyal, S. J. *Carbohydr. Res.* **1979**, *77*, 37. (i) Evdokimov, A. G.; Kalb (Gilboa), A. J.; Koetzle, T. F.; Klooster, W. T.; Martin, J. M. L. *J. Phys. Chem. A* **1999**, *103*, 744.

(8) (a) Hoffmann, R. A.; van Wijk, J.; Leeflang, B. R.; Kamerling, J. P.; Altona, C.; Vliegenthart, J. F. G. *J. Am. Chem. Soc*. **1992**, *114*, 3710. (b) Cros, S.; Imberty, A.; Bouchemal, N.; Hervé du Penhoat, C.; Pérez, S. *Biopolymers* **1994**, *34*, 1433. (c) Radha, A.; Chandrasekaran, R. *Carbohydr. Res.* **1997**, *298*, 105. (d) Chandrasekaran, R.; Radha, A.; Lee, E. J.; Zhang, M. *Carbohydr. Polym.* **1994**, *25*, 235. (e) D'Souza, F. W.; Ayers, J. D.; McCarren, P. R.; Lowary, T. L. *J. Am. Chem. Soc.* **2000**, *122*, 1251. (f) Duker, J. M.; Serianni, A. S. *Carbohydr. Res.* **1993**, *249*, 281. (g) Tran, V. H.; Brady, J. W. *Biopolymers* **1990**, *29*, 961. (h) Tran, V. H.; Brady, J. W. *Biopolymers* **1990**, *29*, 977. (i) Hervé du Penhoat, C.; Imberty, A.; Roques, N.; Michon, V.; Mentech, J.; Descotes, G.; Pérez, S. *J. Am. Chem. Soc.* **1991**, *113*, 3720. (j) Timmermans, J. W.; de Wit, D.; Tournois, H.; Leeflang, B. R.; Vliegenthart, J. F. G. *J. Carbohydr. Chem.* **1993**, *12*, 969. (k) Waterhouse, A. L.; Calub, T. M.; French, A. D. *Carbohydr. Res*. **1991**, *217*, 29. (l) Liu, J.; Waterhouse, A. L.; Chatterton, N. J. *Carbohydr. Res*. **1991**, *217*, 43. (m) Liu, J.; Waterhouse, A. L.; Chatterton, N. J. *J. Carbohydr. Chem.* **1994**, *13*, 859.

(9) (a) French, A. D.; Dowd, M. K. *J. Comput. Chem.* **1994**, *15*, 561. (b) French, A. D.; Dowd, M. K.; Reilly, P. J. *J. Mol. Struct. (THEOCHEM)* **1997**, *395*−*396*, 271. (c) Cassett, F.; Imberty, A.; Herve du Penhoat, C.; Koca, J.; Perez, S. *J. Mol. Struct. (THEOCHEM)* **1997**, *395*−*396*, 211. (d) Cros, S.; du Penhoat, C. H.; Perez, S.; Imberty, A. *Carbohydr. Res.* **1993**, *248*, 81. (e) French, A. D.; Tran, V. *Biopolymers* **1990**, *29*, 1599. (f) Mazeau, K.; Perez, S. *Carbohydr. Res.* **1998**, *311*, 203. (g) Gohlke, H.; Immel, S.; Lichtenthaler, F. W. *Carbohydr. Res.* **1999**, *321*, 96. (h) Immel, S.; Schmitt, G. E.; Lichtenthaler, F. W. *Carbohydr. Res.* **1998**, *313*, 91. (i) Gruza, J.; Koca, J.; Perez, S.; Imberty, A. *J. Mol. Struct. (THEOCHEM)* **1998**, *424*, 269. (j) French, A. D.; Schafer, L.; Newton, S. Q. *Carbohydr. Res.* **1993**, *239*, 51. (k) French, A. D.; Mouhous-Riou, N.; Pérez, S. *Carbohydr. Res.* **1993**, *247*, 51. (l) Calub, T. M.; Waterhouse, A. L.; French, A. D. *Carbohydr. Res.* **1990**, *207*, 221. (m) Dowd, M. K.; Reilly, P. J.; French, A. D. *J. Carbohydr. Chem* **1993**, *12*, 449. (n) Waterhouse, A. L.; Horváth, K.; Liu, J. *Carbohydr. Res*. **1992**, *235*, 1. (o) McCarren, P. R.; Gordon, M. T.; Lowary, T. L.; Hadad, C. M. *J. Phys. Chem. A* **2001**, *105*, 5911.

(10) (a) Serianni, A. S.; Chipman, D. M. *J. Am. Chem. Soc.* **1987**, *109*, 5297. (b) Cloran, F.; Carmichael, I.; Serianni, A. S. *J. Phys. Chem. A* **1999**, *103*, 3783. (c) Ma, B.; Schaefer, H. F., III; Allinger, N. L. *J. Am. Chem. Soc.* **1998**, *120*, 3411. (d) Lii, J.; Ma, B.; Allinger, N. L. *J. Comput. Chem.* **1999**, *20*, 1593. (e) Chung-Phillips, A.; Chen, Y. Y. *J. Phys. Chem. A* **1999**, *103*, 953. (f) Gordon, M. T.; Lowary, T. L.; Hadad, C. M. *J. Am. Chem. Soc.* **1999**, *121*, 9682. (g) Gordon, M. T.; Lowary, T. L.; Hadad, C. M. *J. Org. Chem.* **2000**, *65*, 4954. (h) Foloppe, N.; MacKerell, A. D., Jr. *J. Phys. Chem. B* **1998**, *102*, 6669. (i) Evdokimov, A. G.; Martin, J. M. L.; Kalb (Gilboa), A. J. *J. Phys. Chem. A* **2000**, *104*, 5291. (j) Carmichael, I.; Chipman, D. M.; Podlasek, C. A.; Serianni, A. S. *J. Am. Chem. Soc.* **1993**, *115*, 10863.

(11) Pérez, S.; Imberty, A.; Engelsen, S. B.; Gruza, J.; Mazeau, K.; Jimenez-Barbero, J.; Poveda, A.; Espinosa, J.-F.; van Eyck, B. P.; Johnson, G.; French, A. D.; Kouwijzer, M. L. C. E.; Grootenuis, P. D. J.; Bernardi, A.; Raimondi, L.; Senderowitz, H.; Durier, V.; Vergoten, G.; Rasmussen, K. *Carbohydr Res.* **1998**, *314*, 141.

(12) (a) Csonka, G. I.; Éliás, K.; Csizmadia, I. G. *J. Comput. Chem.* **1997**, *18*, 330. (b) Csonka, G. I.; Éliás, K.; Kolossváry, I.; Sosa, C. P.; Csizmadia, I. G. *J. Phys. Chem. A* **1998**, *102*, 1219. (c) Csonka, G. I.; Kolossváry, I.; Császár, P.; Éliás, K.; Csizmadia, I. G. *J. Mol. Struct. (THEOCHEM)* **1997**, *395*, 29. (d) Csonka, G. I.; Sosa, C. P. *J. Phys. Chem. A* **2000**, *104*, 7113. (e) Csonka, G. I.; Sosa, C. P.; Csizmadia, I. G. *J. Phys. Chem. A* **2000**, *104*, 3381.

(13) We attempted to use the parameter set developed by Homans (Homans, S. W. *Biochemistry* **1990**, *29*, 9110); however, this is not possible for furanose ring systems using MacroModel V6.5. We apologize for the statements in our earlier paper (ref 9o) in which we claimed to have used the Homans parameters. Macromodel quietly rejected the Homans input and only the AMBER* force field was utilized.

(14) (a) MacroModel V6.5: Mohamadi, F.; Richards, N. G. J.; Guida, W. C.; Liskamp, R.; Lipton, M.; Caulfield, C.; Chang, G.; Hendrickson, T.; Still, W. C. *J. Comput. Chem.* **1990**, *11*, 440. (b) Goodman, J.; Still, W. C. *J. Comput. Chem.* **1991**, *12*, 1110.

Chart 1

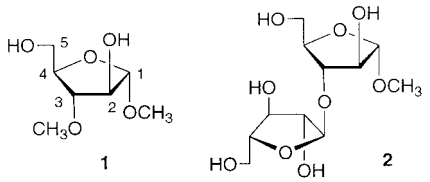

models for aqueous solution. In this way, both twist and envelope conformers are considered, as are all possible exocyclic bond rotamers. Finally, we have used the Boltzmann populations obtained from our computional studies to calculate averaged $^1H-^1H$ coupling constants for **1** and have compared them to $^3J_{H,H}$ measured by ^1H NMR spectroscopy.

To the best of our knowledge, this is the first report of ab initio and DFT computational investigations of a furanoside in which solvation has been addressed. This method should be readily applied to larger systems, including oligosaccharides composed of furanose residues. The molecule chosen for study was methyl 3-*O*-methyl-α-D-arabinofuranoside (**1**; Chart 1), which is a model compound for (1→3)-linked arabinofuranosyl oligosaccharides, e.g., **2** (Chart 1). Polysaccharides containing the glycan moiety of **2** as a constituent are found in the cell wall complex of mycobacteria, including *Mycobacterium tuberculosis*.[2]

Methods

I. Computational Studies. A. Molecular Mechanics Geometries. The SPMC search protocol available in MacroModel Version 6.5[14] was used to generate an initial family of 20 000 conformers of **1**, which is 4 times the total number of possible unique conformations (assuming a single puckering amplitude). Each conformer was then minimized in the gas phase using the AMBER* force field.[13] This generated 348 unique conformers, all of which were within 16 kcal/mol of the global minimum. The geometrical data for these conformers were analyzed using a program (conforMole) that was written by one of us (P.R.M.).[15] The geometries of the lowest energy conformers are provided in the Supporting Information. Each conformer was assigned a number based on its AMBER gas-phase energy and a letter based on its geometry such that the AMBER global minimum is **1a** and the highest energy AMBER conformer is **348a**.

B. Gas-Phase ab Initio Geometries. Semiempirical,[16] ab initio molecular orbital,[17] and density functional theory[18] calculations were performed using Gaussian 98.[19] Many methods were explored for their ability to reduce the number of AMBER conformers requiring HF/6-31G* optimization as discussed in detail in the Supporting Information. First, the 224 AMBER conformers within 8.0 kcal/mol of the global minimum were minimized at the HF/6-31G* level to obtain the most complete HF/6-31G* distribution, which we refer to as the "standard HF/6-31G* distribution". Second, single-point energies of all 348 gas-phase AMBER conformers were determined at the AM1, HF/3-21G, and HF/6-31G* levels;[17] all 348 conformers were also fully optimized at the HF/3-21G level, and the resulting conformers were then reoptimized at the HF/6-31G* level. Third, the standard HF/6-31G* distribution was then compared to the distribution that would have been obtained if the number of conformers was reduced based on energetic criteria at the AMBER, AM1//AMBER, HF/3-21G//AMBER, HF/3-21G//HF/3-21G, or HF/6-31G*//AMBER levels prior to optimization at the HF/6-31G* level.

As discussed in the Supporting Information, these studies allowed us to determine that optimization of only those conformers with HF/6-31G*//AMBER energies within 6 kcal/mol of the global minimum produced a reasonably accurate HF/6-31G* distribution of conformers within 3 kcal/mol of the global minimum (when compared to the HF/6-31G* standard distribution). In the case of **1**, 81 conformers had HF/6-31G*//AMBER energies within 6 kcal/mol of the global minimum, which led to 51 unique conformers following HF/6-31G* optimization. Three of these 51 conformers were eliminated because their HF/6-31G* energies were more than 6 kcal/mol above the global minimum. One other conformer, **90h**, was added to the 48-member family to yield 49 HF/6-31G* conformers. Conformer **90h** had an optimized HF/6-31G* energy of 2.1 kcal/mol above the global minimum, but the HF/6-31G*//AMBER energy was 9.0 kcal/mol above the global minimum. The B3LYP/6-31+G**//HF/6-31G* energy of each of these 49 conformers was calculated. Then, vibrational frequencies of the 12 lowest energy structures were calculated to verify each stationary point as a true minimum.[17] The HF/6-31G* zero-point vibrational energies (ZPEs) were scaled by a factor of 0.9135.[20] The geometry of the lowest energy conformers are provided in the Supporting Information. The conformer numbering is based upon the gas-phase AMBER energies, and the letter designation is "h" for HF/6-31G*.

C. Gas-Phase DFT Geometries. The 49 HF/6-31G* conformers were further minimized at the B3LYP/6-31G* level to yield 46 unique conformers.[21] The geometries of these conformers are provided in the Supporting Information with the AMBER numbering and the letter designation "b" for B3LYP/6-31G*. B3LYP/6-31+G** single-point energies of these 46 conformers were also determined. Vibrational frequencies of the nine lowest energy conformers at the B3LYP/6-31G* level were calculated to verify each as a true minimum, and the ZPEs were scaled by a factor of 0.9806.[20] The vibrational frequency analyses also provided thermal corrections to the enthalpy and entropic corrections so as to determine the relative free energies at 298 K.

To probe the quality of the B3LYP/6-31+G** relative energies, B3LYP/6-311++G(2d,p) single-point energies of the lowest nine optimized B3LYP/6-31G* conformers were determined. MP3/6-31+G** and CCSD/6-31G* single-point energies of these nine conformers were also calculated and then used to estimate the CCSD/6-31+G**//B3LYP/6-31G* energies of each conformer according to eqs 1 and 2.[17,22]

$$\Delta\mathrm{CCSD} = E_{\mathrm{CCSD/6-31G^*}} - E_{\mathrm{MP3/6-31G^*}} \quad (1)$$

$$E_{\mathrm{CCSD/6-31+G^{**}}} = \Delta\mathrm{CCSD} + E_{\mathrm{MP3/6-31+G^{**}}} \quad (2)$$

D. Aqueous-Phase ab Initio Geometries. The geometries of the 49 lowest energy gas-phase HF/6-31G* conformers were further refined using the MN-GSM solvation model developed at the University of Minnesota.[23] This resulted in 48 unique SM5.42/HF/6-31G* aqueous-phase conformers, which are denoted as "sh" (solvated HF/6-31G*) in the Supporting Information. The aqueous-phase B3LYP/6-31+G**//

(15) ConforMole, P. R. McCarren, The Ohio State University. This program is available upon request.

(16) Dewar, M. J. S.; Zoebisch, E. G.; Healy, E. F. *J. Am. Chem. Soc.* **1985**, *107*, 3902.

(17) Hehre, W. J.; Radom, L.; Schleyer, P. v. R.; Pople, J. A. *Ab initio Molecular Orbital Theory*; John Wiley & Sons: New York, 1986.

(18) (a) Labanowski, J. W.; Andzelm, J. *Density Functional Methods in Chemistry*; Springer: New York, 1991. (b) Parr, R. G.; Yang, W. *Density Functional Theory in Atoms and Molecules*; Oxford University Press: New York, 1989.

(19) Frisch, M. J.; Trucks, G. W.; Schlegel, H. B.; Scuseria, G. E.; Robb, M. A.; Cheeseman, J. R.; Zakrzewski, V. G.; Montgomery, J. A., Jr.; Stratmann, R. E.; Burant, J. C.; Dapprich, S.; Millam, J. M.; Daniels, A. D.; Kudin, K. N.; Strain, M. C.; Farkas, O.; Tomasi, J.; Barone, V.; Cossi, M.; Cammi, R.; Mennucci, B.; Pomelli, C.; Adamo, C.; Clifford, S.; Ochterski, J.; Petersson, G. A.; Ayala, P. Y.; Cui, Q.; Morokuma, K.; Malick, D. K.; Rabuck, A. D.; Raghavachari, K.; Foresman, J. B.; Cioslowski, J.; Ortiz, J. V.; Stefanov, B. B.; Liu, G.; Liashenko, A.; Piskorz, P.; Komaromi, I.; Gomperts, R.; Martin, R. L.; Fox, D. J.; Keith, T.; Al-Laham, M. A.; Peng, C. Y.; Nanayakkara, A.; Gonzalez, C.; Challacombe, M.; Gill, P. M. W.; Johnson, B.; Chen, W.; Wong, M. W.; Andres, J. L.; Gonzalez, C.; Head-Gordon, M.; Replogle, E. S.; Pople, J. A. *Gaussian 98*, revision A.7; Gaussian, Inc.; Pittsburgh, PA, 1998.

(20) Scott, A. P.; Radom, L. *J. Phys. Chem.* **1996**, *100*, 16502.

(21) (a) Becke, A. D. *Phys. Rev. A* **1988**, *38*, 3098. (b) Becke, A. D. *J. Chem. Phys.* **1993**, *98*, 5648. (c) Lee, C.; Yang, W.; Parr, R. G. *Phys. Rev. B* **1988**, *37*, 785.

(22) (a) Bartlett, R. J.; Purvis, G. D. *Int. J. Quantum Chem.* **1978**, *14*, 561. (b) Purvis, G. D.; Bartlett, R. J. *J. Chem. Phys.* **1982**, *76*, 1910. (c) Scuseria, G. E.; Janssen, C. L.; Schaefer, H. F., III. *J. Chem. Phys.* **1988**, *89*, 7382. (d) Scuseria, G. E.; Schaefer, H. F., III. *J. Chem. Phys.* **1989**, *90*, 3700.

Chart 2

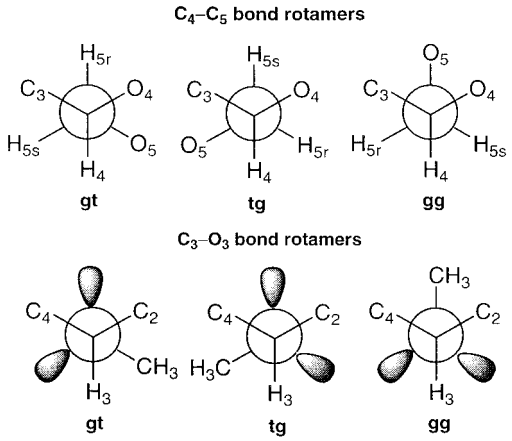

SM5.42/HF/6-31G* energies of these conformers were determined according to eqs 3 and 4 (X = HF) using the gas-phase HF/6-31G* and B3LYP/6-31+G** single-point energies with the solution geometries.

$$\Delta G_{\text{solvation}} = E_{\text{SM5.42/X/6-31G*}} - E_{\text{X/6-31G*(gas)}} \quad (3)$$

$$E_{\text{B3LYP/6-31+G**//SM5.42/X/6-31G*(solution)}} = E_{\text{B3LYP/6-31+G**//SM5.42/X/6-31G*(gas)}} + \Delta G_{\text{solvation}} \quad (4)$$

Vibrational frequency analysis (via numerical differentiation) of the 26 lowest energy SM5.42/HF/6-31G* conformers verified that 24 of the conformers were true minimums. The two conformers that were transition states were not significant contributors to the Boltzmann distribution; however, attempts to identify nearby fully relaxed unique conformers were unsuccessful.

E. Aqueous-Phase DFT Geometries. The geometries of the 46 gas-phase B3LYP/6-31G* conformers were further refined with the MN-GSM aqueous solvation model at the SM5.42/BPW91/6-31G* level.[23] This resulted in 45 aqueous-phase DFT conformers, which are denoted "sb" (solvated BPW91/6-31G*) in the Supporting Information. The solution-phase B3LYP/6-31+G**//SM5.42/BPW91/6-31G* single-point energy of each of these conformers was determined according to eqs 3 and 4 (X = BPW91) using the gas-phase BPW91/6-31G* and B3LYP/6-31+G** energies with the solution geometries. Vibrational frequency analyses of the 12 lowest energy conformers found that most conformers were reasonably well converged; however, some were not. One of the conformers was found to be a transition state, but due to the high cost of these calculations and the minor contribution of this conformer to the Boltzmann distribution (<1%), this was not pursued further.

II. NMR Studies. The conformational preferences of **1** in D_2O were determined by analysis of $^3J_{H,H}$ coupling constants acquired at 800 MHz. These coupling constants were analyzed by PSEUROT 6.2[24] to determine the northern and southern ring conformations in solution. The relative population of each C_4-C_5 rotamer (Chart 2) was determined as previously reported[7a,8e] by analysis of $^3J_{H4,H5}$ and $^3J_{H4,H5'}$. The relative population of each rotamer about the C_3-O_3 bond was probed by two methods. First, measurement of the NOE from the O_3-methyl group hydrogens to H_2 and H_4 provided a general idea of which rotamer was preferred. Second, the $^3J_{COCC}$ coupling from the 3-*O*-methyl carbon to C_2 and C_4 was measured using methyl 3-*O*-[^{13}C]-methyl-α-D-arabinofuranoside([^{13}C]-**1**). These coupling constant data were analyzed using eqs 5−7,

$$1.03X_{gg} + 3.65X_{gt} + 1.03X_{tg} = {}^3J_{C,C4} \quad (5)$$

$$1.03X_{gg} + 1.03X_{gt} + 3.65X_{tg} = {}^3J_{C,C2} \quad (6)$$

$$X_{gg} + X_{gt} + X_{tg} = 1 \quad (7)$$

where X_{gg}, X_{gt}, and X_{tg}, are the populations for the gg, gt, and tg rotamers, respectively (see Chart 2 for definitions). The coefficients in eqs 5 and 6 correspond to the $^3J(60°)$ and $^3J(180°)$ as determined using an experimentally derived Karplus equation for $^3J_{COCC}$.[25] The ^{1}H−^{1}H and ^{13}C−^{13}C coupling constants used in these calculations and details of the synthesis of **1** and [^{13}C]-**1** are provided in the Supporting Information.

Results

I. Generation of Starting Geometries for the ab Initio Studies. Monte Carlo Search and Molecular Mechanics Geometry Optimizations. The starting conformations for the ab initio studies of **1** were generated using a Monte Carlo protocol available in MacroModel;[14] 348 unique AMBER conformers were obtained from an initial 20 000 conformers. The purpose of the conformational search was to generate a library of conformers that possessed a large degree of geometrical diversity. An analysis of the geometrical data indicated that this goal was achieved. For a given ring conformer (e.g., E_4), all three rotamers around each of the exocyclic bonds were represented, typically in equivalent numbers. There were, however, portions of the pseudorotational itinerary that contained no conformers. Figure 2a illustrates the absence of conformers in the region of the pseudorotational itinerary from $P = 135-230°$ (where P is the pseudorotational phase angle).[3a]

The lack of complete coverage of the pseudorotational itinerary was alarming because conformations in this $P = 135-230°$ region are known to be populated by α-D-arabinofuranose rings in solution.[8e] Three possible causes leading to the absence of conformers in this region were considered and are discussed in detail in the Supporting Information. We propose that although there are conformers within this region of the pseudorotational itinerary within 5 kcal/mol of the global minimum, they reside in shallow energy wells for which neither AMBER*,[13] MM2,[26] MM3,[27] nor Hartree−Fock (HF) energy minimization methods are able to isolate easily.

II. Gas-Phase ab Initio Geometries. A. HF/6-31G* Optimization of All Conformers within 8 kcal/mol of the Global Minimum. The AMBER protocol described above generated 294 conformers within 10 kcal/mol of the global minimum. It was clearly desirable to reduce the number of conformers prior to optimization with DFT and the solvation models. HF calculations on carbohydrates with relatively small basis sets (e.g., 6-31G*) have previously been reported to yield accurate energetic information in less computational time than comparable DFT calculations.[10d,12a−c] Therefore, the next objective was to develop a method by which a smaller number of the AMBER conformers could be identified for further study first with the HF/6-31G* method and subsequently with DFT methods and solvation models.

As mentioned in the Introduction, no force field has been specifically parametrized for *O*-furanosides. We were therefore

(23) (a) Xidos, J. D.; Li, J.; Hawkins G. D.; Liotard, D. A.; Cramer, C. J.; Truhlar, D. G.; Frisch, M. J. *MN-GSM*, version 99.2; University of Minnesota: Minneapolis, MN 55455. (b) Li, J.; Zhu, T.; Cramer, C. J.; Truhlar, D. G. *J. Phys. Chem. A* **1998**, *102*, 1820. (c) Li, J.; Hawkins, G. D.; Cramer, C. J.; Truhlar, D. G. *Chem. Phys. Lett.* **1998**, *288*, 293. (d) Zhu, T.; Li, J.; Hawkins, G. D.; Cramer, C. J.; Truhlar, D. G. *J. Chem. Phys.* **1998**, *109*, 9117. (e) Li, J.; Zhu, T.; Hawkins, G. D.; Winget, P.; Liotard, D. A.; Cramer, C. J.; Truhlar, D. G. *Theor. Chem. Acc.* **1999**, *103*, 9.

(24) (a) *PSEUROT 6.2*; Gorlaeus Laboratories: University of Leiden. (b) de Leeuw, F. A. A. M.; Altona, C. *J. Comput. Chem.* **1983**, *4*, 428. (c) Altona, C. *Recl. Trav. Pays-Bas* **1982**, *101*, 413.

(25) Bose, B.; Zhao, S.; Stenutz, R.; Cloran, F.; Bondo, P. B.; Bondo, G.; Hertz, B.; Carmichael, I.; Serianni, A. S. *J. Am. Chem. Soc.* **1998**, *120*, 11158.

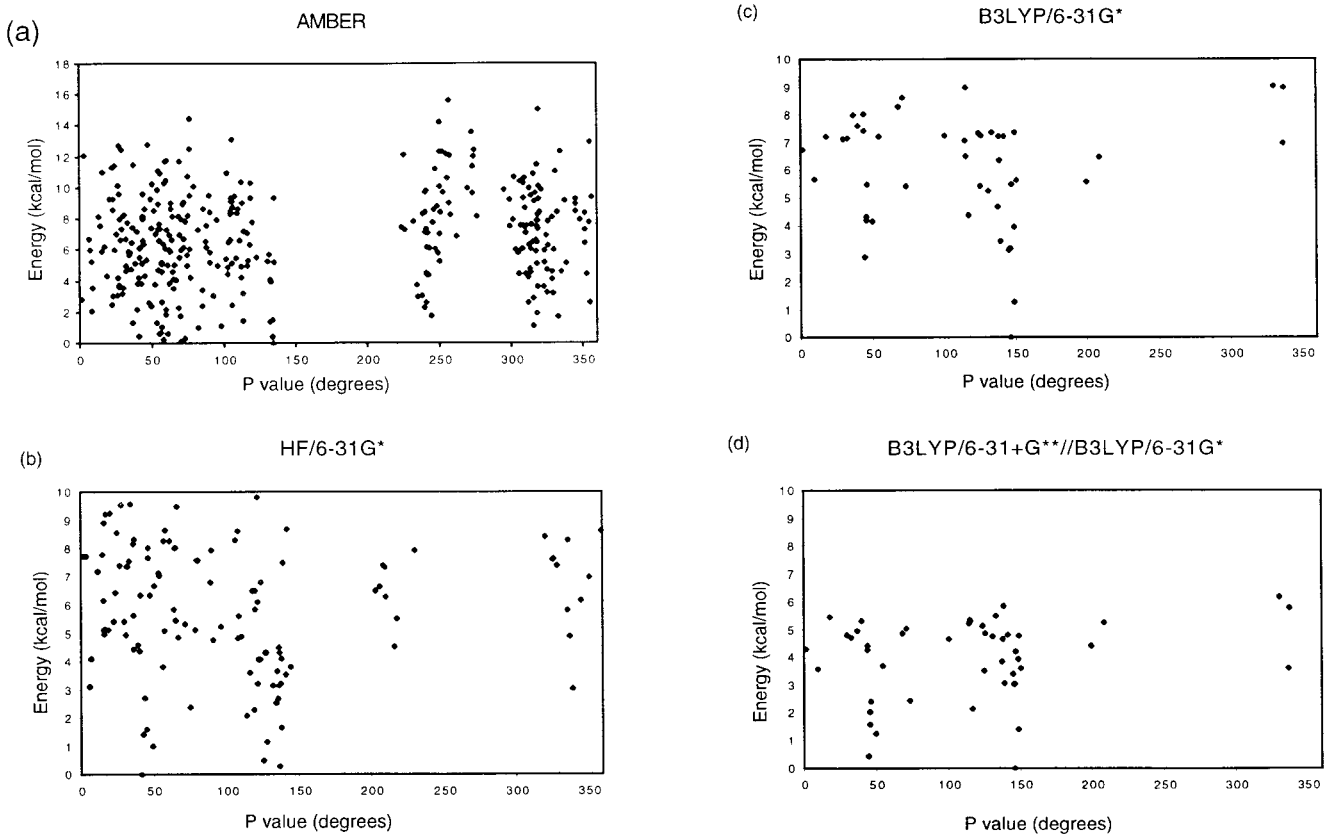

Figure 2. (a) Distribution of conformers of **1** following AMBER optimization of the Monte Carlo search generated structures. Each of the 348 conformers is identified by a diamond. (b) Distribution of conformers of **1** following HF/6-31G* optimization of the 224 AMBER conformers with energies within 8 kcal/mol of the global minimum. A total of 125 conformers were identified. (c) Distribution of conformers of **1** following B3LYP/6-31G* optimization of the 49 HF/6-31G* conformers with HF/6-31G* energies below 6 kcal/mol. A total of 46 conformers were identified. (d) Distribution of conformers of **1** following B3LYP/6-31+G** single-point energy calculations with the 46 B3LYP/6-31G* conformers.

concerned that reducing the number of conformers by having used a low-energy cutoff based on AMBER relative energies alone might have resulted in the loss of conformers that would be important at higher levels of theory. Accordingly, a number of methods were explored for reducing the number of AMBER conformers carried on for further study, which are discussed in the Supporting Information. However, it was first necessary to have a standard against which these methods could be compared. We chose to generate this standard by optimizing (HF/6-31G*) the geometry of all 224 AMBER conformers within 8 kcal/mol of the global minimum. This cutoff was chosen because this number of HF/6-31G* optimizations was deemed feasible with the resources available and because we felt that any conformers important for the Boltzmann distribution at higher levels of theory would lie within this energy window in the AMBER distribution.

These HF/6-31G* optimizations produced 125 unique conformers (the "HF/6-31G* standard distribution"). Representation of the three rotamers about each exocyclic bond was similar to that seen in the AMBER conformers. There was, however, a significant shift in the distribution of ring conformers across the pseudorotational itinerary (Figure 2b). First, the region from $P = 135-230°$ which was unrepresented in the AMBER surface was replaced by two smaller "empty" regions ($P = 145-200°$ and $255-320°$). Furthermore, whereas nearly 40% of the 224 AMBER conformers were on the western portion ($P = 180-360°$) of the pseudorotational itinerary, only 20% of the conformers were in this region after refinement at the HF/6-31G* level of theory. The HF/6-31G* optimized conformers with $P > 180°$ were also of significantly higher energy than those with a pseudorotational angle less than 180°. This is expected given that, in these western conformers, the C_4 hydroxymethyl group is pseudoaxial and the C_1 methoxy group is pseudoequatorial. Whereas no clear minimum could be identified in the AMBER distribution, major northern ($^3T_4$) and southern ($^2T_1$) minimums could be identified in the HF/6-31G* family of conformers.

B. Development of a Method To Decrease the Number of Required HF/6-31G* Optimizations. Generation of the HF/6-31G* standard distribution required the optimization of 224 AMBER conformers. In order for this protocol to be practical for use on larger oligofuranosides, it was necessary to develop a relatively inexpensive method for reducing the number of AMBER conformers requiring HF/6-31G* optimization without significantly compromising the accuracy of the results. Five methods were evaluated as a means to decrease the number of conformers carried on for further study. In addition to the AMBER energies, HF/6-31G* single-point energies, AM1 single-point energies, HF/3-21G single-point energies, and HF/3-21G optimized energies were calculated for all 348 AMBER conformers (Table 1). The effectiveness of each method was evaluated by determining the number of calculations that would be required to obtain a distribution of final conformers that was similar to the "HF/6-31G* standard distribution". As discussed in the Supporting Information, *these results indicated that the most practical and secure method for reducing the number of required HF/6-31G* optimizations was to optimize only those AMBER conformers with an HF/6-31G*//AMBER energy within 6 kcal/mol of the global minimum*. In the case of **1**, the 6 kcal/mol energy cutoff would reduce the number of HF/6-31G*

Table 1. Comparison of Methods Explored To Reduce the Number of Required HF/6-31G* Optimizations

energy method	energy cutoff (kcal/mol)	geometry	no. of HF/6-31G* optimizations	% of HF/6-31G* conformers found[a]	no. of structures missing[b] <3 kcal/mol	no. of structures missing[b] <5 kcal/mol
AMBER[c]	8.0	AMBER	224	100	0	0
AMBER	6.0	AMBER	134	57	0	2
AMBER	5.0	AMBER	95	46	0	7
HF/6-31G*	10.0	AMBER	243	90	0	0
HF/6-31G*	8.0	AMBER	162	67	1	3
HF/6-31G*	**6.0**	**AMBER**	**81**	**41**	**1**	**4**
HF/6-31G*	4.0	AMBER	31	17	1	23
AM1	8.0	AMBER	238	85	0	0
AM1	6.0	AMBER	144	59	1	5
HF/3-21G	10.0	AMBER	84	41	1	9
HF/3-21G	10.0	HF/3-21G	75	51	3	11

[a] Percentage found at the different theoretical levels as compared to the 125 conformers of the HF/6-31G* standard distribution, which was found by optimizing all structures with $E_{AMBER} < 8$ kcal/mol. [b] Compared to the 125 conformers of the HF/6-31G* standard distribution, which was found by optimizing all structures with $E_{AMBER} < 8$ kcal/mol. [c] HF/6-31G* standard distribution.

optimizations required to 81 with a loss of only 4 conformers within 5 kcal/mol of the global minimum compared to the HF/6-31G* standard distribution.[28] Optimization (HF/6-31G*) of these 81 conformers yielded 51 unique conformers. Three of the HF/6-31G* optimized conformers had energies greater than 6 kcal/mol above the global minimum; these were discarded to yield 48 unique conformers. This does not include one conformer, **90h**, that was present in the HF/6-31G* standard distribution and that had an HF/6-31G*//HF/6-31G* energy of 2.1 kcal/mol above the global minimum; its HF/6-31G*//AMBER energy was 9.0 kcal/mol. This conformer was included in all future studies but proved to be only a minor contributor to the Boltzmann distribution at each level of theory studied. The HF/6-31G* conformers that contribute to the Boltzmann distribution and their energies are shown in Figure 3.

C. B3LYP/6-31+G Single-Point Energies.** Previous and current work in our group has demonstrated that the best relative energies for HF/6-31G* geometries on similar systems is at the B3LYP/6-31+G**//HF/6-31G* level of theory, even when compared to G2(MP2) and CBS-QB3 energies.[10g,29] Therefore, the B3LYP/6-31+G** single-point energies of the 49 lowest energy HF/6-31G* conformers were determined.

III. Gas-Phase Density Functional Theory Geometries. A. B3LYP/6-31G* Optimizations. The geometries chosen as the starting point for optimization at the B3LYP/6-31G* level were the 49 HF/6-31G* conformers within 6 kcal/mol of the global minimum. Greater diversity could have been achieved by starting from the 81 AMBER conformers with an HF/6-31G*//AMBER energy within 6 kcal/mol of the global minimum. However, this would have been more expensive by almost a factor of 2. Optimization of the 49 HF/6-31G* conformers at the B3LYP/6-31G* level resulted in 46 conformers that maintained the high degree of structural diversity seen in the HF/6-31G* conformers. The primary difference between the HF/6-31G* and B3LYP/6-31G* conformers was an increase of the average bond distances. The average C−C bond distance increased by 0.009 Å upon optimization at the B3LYP/6-31G* level. This correlates well with previous reports that bond lengths in furanose rings calculated by DFT methods are 0.4−1.9% larger than those from the Hartree−Fock method.[10b] The relative energies of the conformers, however, changed markedly. Conformers that were stabilized by strong intramolecular hydrogen bonding (southern hemisphere conformers) decreased in energy at the B3LYP/6-31G* level as compared to those that lacked strong hydrogen bonding (northern hemisphere conformers) (Figure 2c). It has previously been noted[12,10c,d,g,30] that B3LYP/6-31G* energies of carbohydrates and other molecules capable of extensive intramolecular hydrogen bonding are inaccurate due to an overestimation of these interactions. These errors in the B3LYP/6-31G* energies can be compensated for by the use of more flexible basis sets with diffuse functions. Accordingly, we next determined single-point energies using a larger basis set.

B. B3LYP/6-31+G Single-Point Energies.** It has previously been demonstrated for arabinofuranosides that *virtually identical geometries* are attained by optimization at the B3LYP/6-31+G** or B3LYP/6-31G* levels.[10g] Use of the larger basis set, however, reduces the overestimation of hydrogen bonding as the energy is more sensitive to the basis set than is the geometry.[17] Therefore, B3LYP/6-31+G** single-point energies of the 46 fully optimized B3LYP/6-31G* conformers were calculated. The B3LYP/6-31+G**//B3LYP/6-31G* energies resulted in a distribution of conformers (Figure 2d) whose North/South relative energies were similar to those obtained at the HF/6-31G* level of theory (Figure 2b). Previous work on arabinofuranosides has shown that the B3LYP/6-31+G**//B3LYP/6-31G* energies compare favorably to those obtained with even more flexible basis sets.[10g] This was also illustrated for **1** by calculating B3LYP/6-311++G(2d,p) single-point energies of the nine lowest energy B3LYP/6-31+G**//B3LYP/6-31G* conformers (Figure 4). As illustrated in Table 2, the relative energies were not significantly altered by the increase in basis set size. Therefore, the B3LYP/6-31+G**//B3LYP/6-31G* energies were used to determine which conformers to study further.

C. Free Energy Calculations. The Gibbs free energy contributions of the nine conformers shown in Figure 4 were determined (Table 3). The effect of including just the enthalpy correction at room temperature is also shown. Southern conformers **1b** and **5b** suffered a greater entropic penalty than the northern conformers as shown by the decreased relative energies

(26) Allinger, N. L. *J. Am. Chem. Soc.* **1977**, *99*, 8127.

(27) Allinger, N. L.; Yuh, Y. H.; Lii, J.-H. *J. Am. Chem. Soc.* **1989**, *111*, 8551.

(28) An 8 kcal/mol cutoff for the HF/6-31G*//AMBER energy would have required optimizing 162 conformers. This would have resulted in the loss of three conformers with optimized energies of <5 kcal/mol (compared to the HF/6-31G* standard distribution) and one conformer within 3 kcal/mol of the global minimum. Of the 162 AMBER conformers requiring HF/6-31G* optimization, only 14 had an AMBER energy greater than 8 kcal/mol. Optimization of these 14 conformers yielded 9 unique conformers that were not present in the HF/6-31G* standard distribution, but each had an energy greater than 6 kcal/mol above the HF/6-31G* global minimum.

(29) Callam, C. S.; Singer, S. J.; Lowary, T. L.; Hadad, C. M. *J. Am. Chem. Soc.*, submitted.

(30) Del Bene, J. E.; Person, W. B.; Szczepaniak, K. *J. Phys. Chem.* **1995**, *99*, 10705.

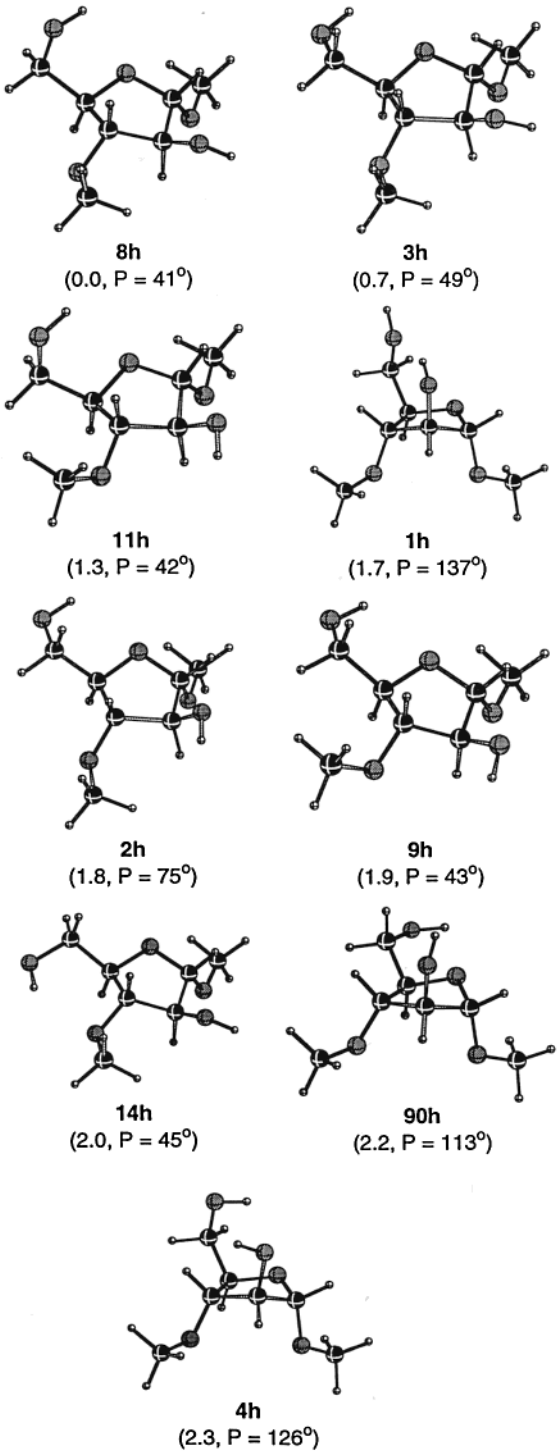

Figure 3. Optimized HF/6-31G* conformers of **1** contributing to the Boltzmann distribution in the gas phase. The left number is the relative Gibbs free energy at 298 K (in kcal/mol); the right number is the pseudorotational phase angle (*P*) of the conformer as defined in ref 3a.

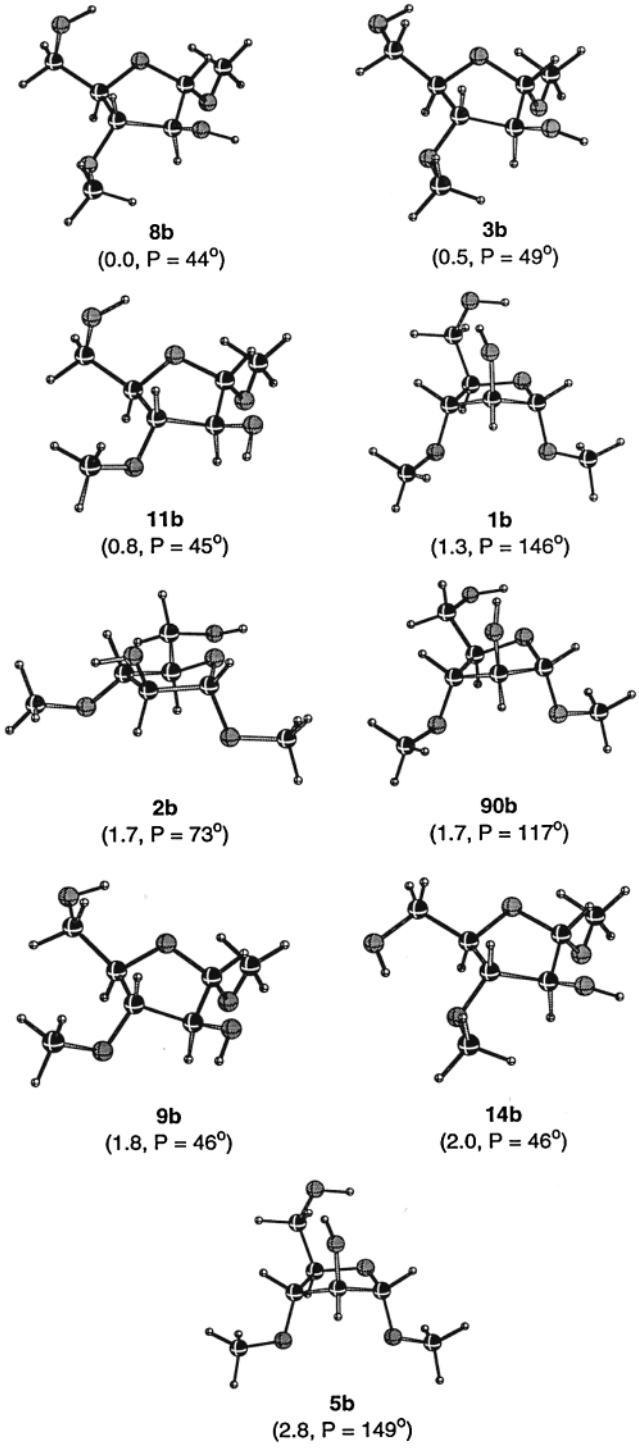

Figure 4. Optimized B3LYP/6-31G* conformers of **1** contributing to the Boltzmann distribution in the gas phase at the B3LYP/6-31+G**//B3LYP/6-31G* level of theory. The left number is the relative Gibbs free energy at 298 K (in kcal/mol); the right number is the pseudorotational phase angle (*P*) of the conformer as defined in ref 3a.

of the northern conformers (**2b**, **3b**, **8b**, **9b**, **11b**, **14b**). These results can be explained in terms of hydrogen bonding (Table 4). The southern conformers have a strong intramolecular $O_2-H\cdots O_5$ hydrogen bond as well as a weak $O_5-H\cdots O_4$ hydrogen bond. This hydrogen-bonding network requires a more ordered system than the northern conformers, which have only one intramolecular H-bond ($O_5-H\cdots O_4$). Among the northern conformers, all had similar entropic penalties, except **14b**. The C_4-C_5 bond in this conformer adopted the tg orientation, which makes possible an $O_5-H\cdots O_3$ hydrogen bond that is stronger (i.e., shorter and more linear[31]) than the $O_5H\cdots O_4$ hydrogen bonds present in the other northern conformers.

D. CCSD/6-31+G Single-Point Energies.** We had hoped to obtain CCSD(T)/6-31+G*//B3LYP/6-31G* energies of the nine lowest energy conformers (Figure 4) to compare with the B3LYP/6-31+G**//B3LYP/6-31G* energies. We anticipated

(31) Jeffrey, G. A. *An Introduction to Hydrogen Bonding*; Oxford Press: New York, 1997; pp 11−32.

Table 2. Energies of Conformers Contributing to the Gas-Phase Boltzmann Distribution at a Number of Levels of Theory[a,b]

		conformer								
basis set	method	**1b**	**2b**	**3b**	**5b**	**8b**	**9b**	**11b**	**14b**	**90b**
6-31G*	HF	0.0	2.5	1.1	1.4	0.2	2.9	1.8	1.9	2.3
6-31G*	MP2	0.0	7.2	6.1	1.6	4.4	7.6	5.9	5.8	5.0
6-31G*	MP3	0.0	5.8	4.7	1.5	3.3	6.2	4.7	4.6	4.4
6-31G*	CCSD	0.0	6.0	4.9	1.5	3.4	6.5	4.8	4.8	4.4
6-31G*	B3LYP	0.0	5.4	4.2	1.3	2.9	5.5	4.3	4.2	4.4
6-31+G**	HF	1.4	2.0	0.6	2.8	0.0	2.2	1.3	1.9	2.3
6-31+G**	MP2	0.0	4.6	3.4	1.7	2.2	4.7	3.3	3.9	2.8
6-31+G**	MP3	0.0	3.6	2.4	1.6	1.3	3.7	2.4	3.0	2.4
6-31+G**	CCSD	0.0	3.8	2.6	1.6	1.5	4.0	2.5	3.2	2.4
6-31+G**	B3LYP	0.0	2.4	1.2	1.4	0.5	2.4	1.6	2.0	2.1
6-311++G(2d,p)	B3LYP	0.0	2.2	1.2	1.3	0.4	2.4	1.6	2.0	2.0
	P[c]	146	73	49	149	44	46	45	46	117
	ring conformer	$^2T_1$	$^OT_4$	E_4	$^2T_1$	E_4	E_4	E_4	E_4	E_1

[a] The B3LYP/6-31G* geometries were used. [b] Energy in kcal/mol, relative to the bottom of the well. [c] Altona-Sundaralingam pseudorotational phase angle (in degrees) as defined in Reference 3a.

Table 3. Effect of Enthalpy and Entropy Corrections on the B3LYP/6-31G* Energies

conformer no.	ring conformer	family	ΔE_{BW}[a]	ΔH_{298}[b]	ΔG_{298}[c]
1b	$^2T_1$	S	0.0	0.0	0.0
2b	$^OT_4$	N	5.4	5.0	3.5
3b	E_4	N	4.2	3.9	2.2
5b	$^2T_1$	S	1.3	1.3	1.4
8b	E_4	N	2.9	2.6	1.2
9b	E_4	N	5.5	5.2	3.6
11b	E_4	N	4.3	4.0	2.3
14b	E_4	N	4.2	4.0	2.9
90b	E_1	S	4.4	4.1	2.8

[a] Relative bottom-of-the-well energies (kcal/mol) without ZPE, thermal, or entropic corrections. [b] Relative enthalpies (kcal/mol) with (scaled) ZPE and thermal corrections at 298 K. [c] Relative Gibbs free energies (kcal/mol) at 298 K.

Table 4. Hydrogen-Bonding Patterns in the Low-Energy B3LYP/6-31G* Conformers

conformer no.	bond type[a]	bond distance[b]	bond angle[c]
1b	$O_2H\cdots O_5$	1.96	158.2
	$O_5H\cdots O_4$	2.28	105.5
2b	$O_5H\cdots O_4$	2.39	107.1
3b	$O_5H\cdots O_4$	2.39	107.1
5b	$O_2H\cdots O_5$	1.95	158.5
	$O_5H\cdots O_4$	2.27	105.7
8b	$O_5H\cdots O_4$	2.29	110.1
9b	$O_5H\cdots O_4$	2.28	109.6
11b	$O_5H\cdots O_4$	2.33	108.8
14b	$O_5H\cdots O_3$	2.13	141.1
90b	$O_5H\cdots O_4$	2.34	108.6

[a] Hydrogen bond defined as the hydrogen donor···oxygen acceptor. [b] H···O distance given in angstroms. [c] O−H···O angle given in degrees.

that these results would prove the accuracy of the less expensive DFT calculations; however, the CCSD(T) calculations proved impractical.[32] Therefore, we determined CCSD/6-31+G**//B3LYP/6-31G* energies of these conformers by an additivity approximation.[22] By determining the difference between the MP3/6-31G* and the CCSD/6-31G* energies, it was possible to estimate the energy difference between the MP3/6-31+G** and CCSD/6-31+G** energies. As shown in Tables 2 and 5, the CCSD/6-31+G**//B3LYP/6-31G* energies are qualitatively similar to the B3LYP/6-31+G**//B3LYP/6-31G* values.

IV. Aqueous-Phase Studies. A. Ab Initio Geometries. The aqueous-phase Hartree−Fock conformer distribution was determined by optimization of the 49 lowest energy gas-phase HF/6-31G* conformers. The ability of several polarizable continuum models (PCM)[33] to efficiently optimize the geometry of these conformers was examined. The PCM and SCIPCM[34] methods both suffered from dissociation of the C_1-H_1 bond in the early stages of optimization. It was not possible to circumvent this difficulty by varying the number of tesserea, so these methods were abandoned. The CPCM method[35] was also examined, and this method did not suffer from dissociation of the C_1-H_1 bond. The CPCM method was not, however, capable of generating a complete list of well-converged conformers. Therefore, methods based on the PCM approach were abandoned.

Fortunately, the MN-GSM solvation model[23] developed by Cramer, Truhlar, and co-workers at the University of Minnesota was able to efficiently optimize the geometry of the 49 gas-phase HF/6-31G* conformers to yield 48 unique conformers. Vibrational frequency analyses of the 26 conformers within 3 kcal/mol of the global minimum indicated that most of the conformers were fully relaxed structures. From the vibrational frequency analyses, as in the gas-phase calculations, it was determined that the enthalpic and entropic contributions to the Gibbs free energy could be important for the accurate prediction of the conformer distribution of **1**. The 16 conformers with the lowest Gibbs free energy are shown in Figure 5. The solution-phase B3LYP/6-31+G** single-point energy of each conformer was then evaluated as discussed in the Methods section ID. It is unclear whether the SM5.42/HF/6-31G* or B3LYP/6-31+G**//SM5.42/HF/6-31G* relative energies are more accurate for these solution-phase calculations. Furthermore, due to the parametrization of the SM5.42 model, it is also unclear to what extent enthalpic and entropic contributions to the free energy should be included with the bottom-of-the-well energy of the solute. Therefore, the results at both levels of theory, with and without inclusion of the complete thermal and entropic corrections to the Gibbs free energy of the solute, will be discussed below.

(32) For example, even the CCSD/6-31G* single-point energy calculation of each conformer took ~100 h of CPU time on a Silicon Graphics Origin 2000.

(33) Cramer, C. J.; Truhlar, D. G. *Chem. Rev.* **1999**, *99*, 2161.

(34) (a) Tomasi, J.; Persico, M. *Chem. Rev.* **1994**, *94*, 2027. (b) Cossi, M.; Barone, V.; Cammi, R.; Tomasi, J. *Chem. Phys. Lett.* **1996**, *255*, 327. (c) Barone, V.; Cossi, M.; Tomasi, J. *J. Chem. Phys.* **1997**, *107*, 3210. (d) Barone, V.; Cossi, M.; Tomasi, J. *J. Comput. Chem.* **1998**, *19*, 404. (e) Cossi, M.; Barone, V. *J. Chem. Phys.* **1998**, *109*, 6246. (f) Foresman, J. B.; Keith, T. A.; Wiberg, K. B.; Snoonian, J.; Frisch, M. J. *J. Phys. Chem.* **1996**, *100*, 16098. (g) Miertus, S.; Scrocco, E.; Tomasi, J. *Chem. Phys.* **1981**, *55*, 117.

(35) (a) Barone, V.; Cossi, M. *J. Phys. Chem. A* **1998**, *102*, 1995. (b) Klamt, A.; Schueuermann, G. *J. Chem. Soc., Perkin Trans. 2* **1993**, 799.

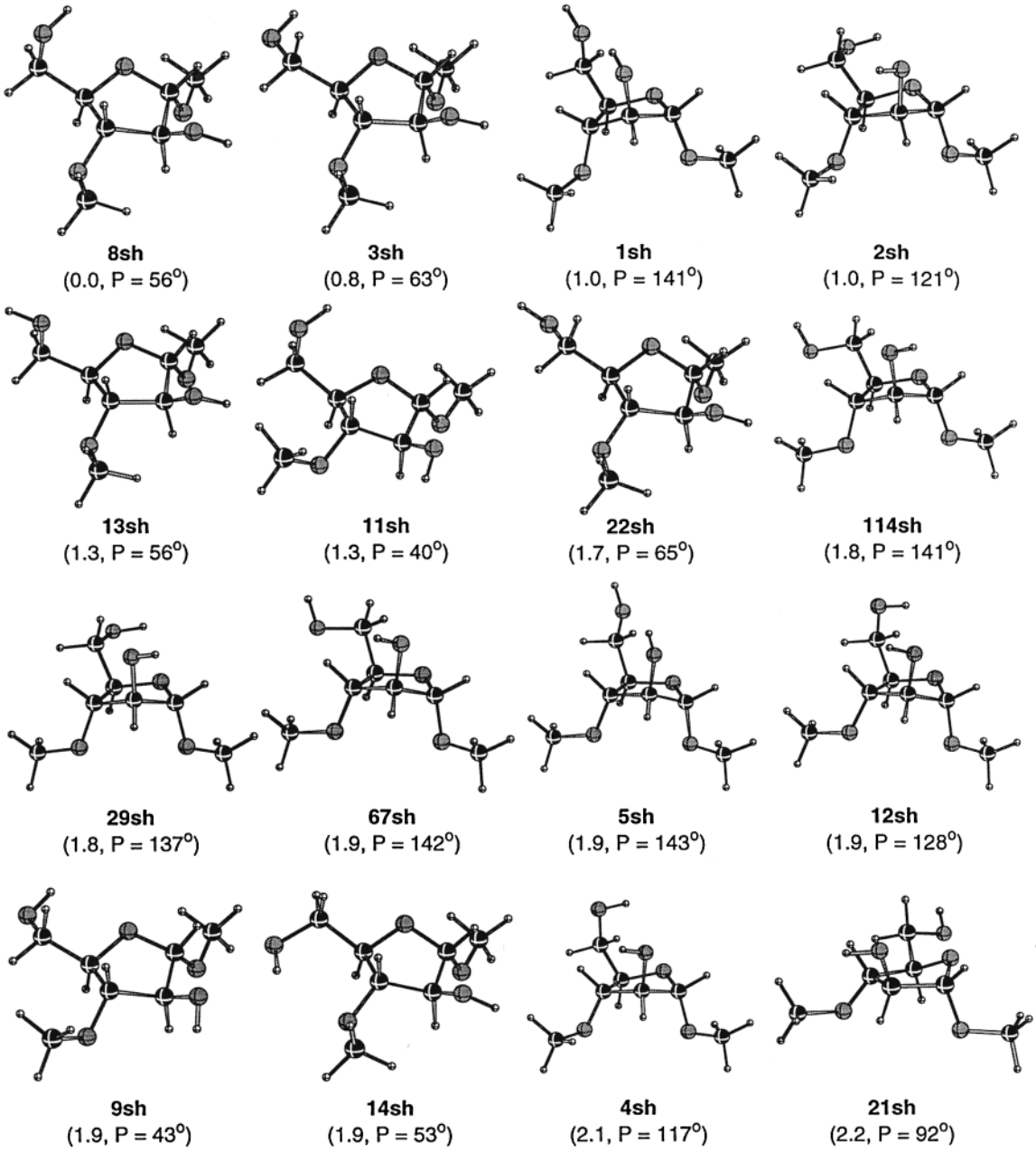

Figure 5. SM5.42/HF/6-31G* conformers of **1** contributing to the Boltzmann distribution in the aqueous phase. The left number is the relative Gibbs free energy at 298 K (in kcal/mol); the right number is the pseudorotational phase angle (*P*) of the conformer as defined in ref 3a.

B. Density Functional Theory Geometries. The MN-GSM solvation model was also used to optimize the 46 gas-phase DFT conformers. With the current implementation, it is not possible to use the B3LYP method with the 6-31G* basis set. Therefore, the SM5.42/BPW91/6-31G* level of theory was used to obtain 45 solution-phase conformers. The aqueous-phase B3LYP/6-31+G** single-point energy of each conformer was then determined as discussed in Methods section IE. Vibrational frequency analysis of the 12 lowest energy conformers indicated that many were not fully converged (but were close for all four convergence criteria). Due to this and the high expense of each of the frequency calculations (~250 CPU hours each), it was not deemed feasible to reoptimize the geometry of these conformers using the calculated force constants. The vibrational frequency analysis was also used to calculate the Gibbs free energy and Boltzmann distribution in aqueous solution at the B3LYP/6-31+G**//SM5.42/BPW91/6-31G* level of theory. The results are discussed below.

Table 5. Gas-Phase Distribution of the Lowest Energy B3LYP/6-31G* Conformers at Various Levels of Theory[a]

conformer no.	ring conformer	family	B3LYP/ 6-31+G**	CCSD/ 6-31+G**
1b	$^{2}T_{1}$	S	6	27
2b	$^{O}T_{4}$	N	3	1
3b	E_4	N	21	10
5b	$^{2}T_{1}$	S	0	1
8b	E_4	N	50	40
9b	E_4	N	2	1
11b	E_4	N	13	11
14b	E_4	N	2	1
90b	E_1	S	3	7

[a] Distributions calculated using relative Gibbs free energies at 298 K.

Discussion

I. NMR Studies. The ring, C_4-C_5, and C_3-O_3 conformational preferences of **1** in aqueous solution were probed by NMR

Table 6. Comparison of the Boltzmann Distribution Calculated for **1** at Various Levels of Theory and from Experiment

			major north *P* family[b]		major south *P* family[b]			C_4-C_5 bond rotamers[c]			C_3-O_3 bond rotamers[c]		
entry	method	phase	P^b	%	P^b	%	N/S	gg	gt	tg	gg	gt	tg
1	ΔE AMBER	gas	E_4	24	$^2T_1$	28	72/28	51	47	2	0	75	25
2	ΔG HF/6-31G*	gas	$^3T_4$	69	E_1	8	84/16	81	17	2	0	92	8
3	ΔG B3LYP/6-31+G**//HF/6-31G*	gas	$^3T_4$	72	$^2T_1$	4	93/7	73	25	2	0	91	9
4	ΔG B3LYP/6-31+G**//B3LYP/6-31G*	gas	E_4	91	$^2T_1$	9	91/9	69	29	2	0	84	16
5	ΔG CCSD/6-31+G**/B3LYP/6-31G*	gas	$^3T_4$	63	$^2T_1$	28	65/35	79	19	2	0	86	14
6	ΔE AMBER	solution	E_4	26	$^2T_1$	33	65/35	60	38	2	0	71	29
7	ΔE SM5.42/HF/6-31G*[a]	solution	E_4	29	$^2T_1$	28	48/52	73	22	5	0	83	17
8	ΔG SM5.42/HF/6-31G*	solution	E_4	50	$^2T_1$	14	74/26	68	28	6	0	84	18
9	ΔE B3LYP/6-31+G**//SM5.42/HF/6-31G*[a]	solution	E_4	31	$^2T_1$	21	72/28	57	41	2	0	89	11
10	ΔG B3LYP/6-31+G**//SM5.42/HF/6-31G*	solution	E_4	23	$^2T_1$	7	86/14	49	49	2	0	87	13
11	ΔE B3LYP/6-31+G**//SM5.42/BPW91/6-31G*[a]	solution	E_4	29	$^2T_1$	25	64/36	61	39	0	0	89	11
12	ΔG B3LYP/6-31+G**//SM5.42/BPW91/6-31G*	solution	$^OT_4$	44	$^2T_1$	5	89/11	47	53	0	0	87	13
13	solution NMR	solution	^OE	70 ± 10	^2E	30 ± 10	70/30	42	37	21	5	68	27

[a] Includes ΔG of solvation, but not ZPE, thermal, or entropic contributions. [b] Altona−Sundaralingam phase angle (in degrees) as defined in ref 3a. [c] See Chart 2 for definitions.

spectroscopy. PSEUROT 6.2 analysis of the $^3J_{H,H}$ of the ring hydrogens indicated that the equilibrium population in solution from the room-temperature data was a 60:40, N/S ratio of the ^OE ($P = 87°$)[36] and $^2T_3$ ($P = 173°$) ring conformations. Due to potential experimental error in the measurement of the $^1H-^1H$ coupling constants, we carried out a series of PSEUROT analyses in which we systematically varied the coupling constants and ring-puckering amplitudes. The range of $^3J_{H,H}$ were ±0.1 Hz of those measured from the NMR spectrum of **1** and puckering amplitudes of 30, 35, and 39° were used. The results of the analysis, which are detailed in the Supporting Information, suggest that $P_N = 88 \pm 4°$, $P_S = 165 \pm 20°$, and the north:south ratio = 70:30 ± 10%. Analysis[7a] of the H_4-H_5 $^3J_{H,H}$ indicated that the C_4-C_5 rotamer distribution in aqueous solution at room temperature was 42% gg, 37% gt, and 21% tg (Chart 2). Finally, the orientation of the O_3-methyl group was probed. NOE experiments showed that irradiation of the O_3-methyl group hydrogens provided stronger NOE enhancement to H_2 (5.2%) than to H_4 (2.1%). This suggests that the preferred orientation of the O_3-methyl group is anti to C_4. Furthermore, analysis of the $^3J_{COCC}$ in [^{13}C]-**1** using eqs 5−7 (Methods Section II) indicated that the 3-*O*-methyl group was 68% anti to C_4 (gt), 27% anti to C_2 (tg), and 5% anti to H_3 (gg) (Chart 2). The $^3J_{COCC}$ values used for these calculations can be found in the Supporting Information. It should be appreciated that the Karplus equation from which eqs 5 and 6 were derived was developed using $^3J_{COCC}$ involving the anomeric carbon, not for other C−O−C−C fragments on carbohydrate rings. Accordingly, these equations are subject to errors. For example, we consider it likely that the population of the gg rotamer, in which the methyl group is under the ring, is less than the 5% listed above. Nevertheless, eqs 5−7 allow us to quantitate the rotamer populations about the C_3-O_3 bond more accurately than if NOE data alone were used.

II. Molecular Mechanics Studies. The gas-phase AMBER Boltzmann distribution of conformers did not compare well with the experimentally observed solution distribution (Table 6, compare entries 1 and 13) as determined by PSEUROT analysis of the $^1H-^1H$ coupling constant data. The conformers for the northern and southern minimums were both too far to the north when compared to the experimentally observed ranges. Despite these inadequacies, however, the gas-phase AMBER level of theory did well in other respects. As shown in Table 6, the north/south ratio found by this level of theory (72:28) correlates well with experiment (70:30). Furthermore, the rotamer populations around the C_4-C_5 and C_3-O_3 exocyclic bonds also compare well with those determined experimentally.

III. Ab Initio Geometries. As expected, the gas-phase HF/6-31G* and B3LYP/6-31+G**//HF/6-31G* Boltzmann distributions of conformers did not compare well with those obtained by PSEUROT analysis of the experimental data from the NMR studies in aqueous solution (Figure 6a−d, Table 6, compare entries 2, 3, and 13). As with the AMBER levels of theory, the northern and southern minimums were shifted significantly north of the observed experimental minimums. The north/south ratio also overestimated the northern preference at both the HF/6-31G* (84:16) and B3LYP/6-31+G**//HF/6-31G* (93:7) levels of theory. The gg rotamer of the C_4-C_5 bond is also too highly favored at both levels of theory compared to experiment. This was an expected consequence of performing gas-phase calculations since the gg rotamer allows stronger hydrogen bonding than the gt and tg rotamers. At both levels of theory, the predicted distribution of rotamers around the C_3-O_3 bond overly favors the rotamer in which the methoxy group is anti to C_4.

The results from the aqueous-phase HF calculations carried out at the SM5.42/HF/6-31G* level of theory were quite encouraging. Significantly, conformers that were stabilized in the gas phase by an $O_5H\cdots O_4$ hydrogen bond maintained the same exocyclic bond rotamers in the aqueous phase, but relaxed such that the H-bonds were longer by ∼0.2 Å and less linear by ∼5°. The northern and southern minimums were still shifted too far to the north in comparison to the experimental results, but agreement with experiment was better when compared to the gas-phase calculations. As shown in Figure 6e−h and Table 6 (compare entries 2, 3, and 7−10), the northern minimums shifted from a $^3T_4$ ring conformer in the gas phase to an E_4 ring conformer in solution. Furthermore, the Boltzmann distributions also contained 2−14% of the ^OE ring conformer, which is the northern conformer predicted by PSEUROT. This ring conformer was not present within ∼5 kcal/mol of the global minimum in the gas-phase distributions. The identity of the southern minimum also shifted closer (south) to the experimentally observed ^2E ring conformer by 5−10°, almost within experimental error. The north/south ratio predicted by each level of theory, with the exception of the bottom-of-the-well SM5.42/HF/6-31G* distribution, is close to that observed experimentally (Table 6, compare entries 7−10). The rotamer populations about the C_4-C_5 and C_3-O_3 bonds at all four levels of theory were closer to those observed experimentally than those in the gas phase (Table 6).

(36) The $P = 87°$ conformer will be denoted as northern, despite also being eastern.

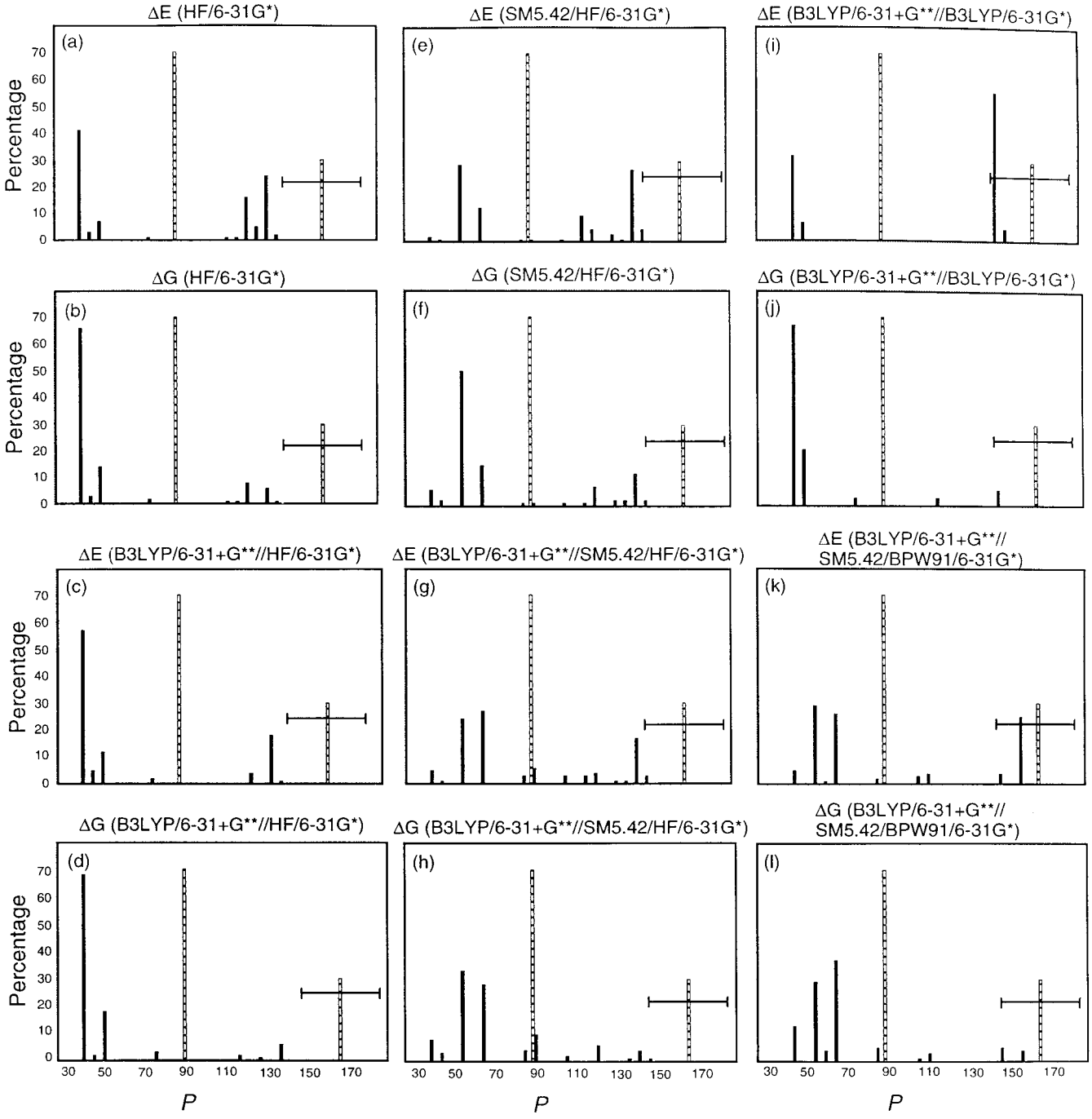

Figure 6. Boltzmann distribution at several levels of theory. Dashed lines represent the experimentally observed distribution in aqueous solution from NMR studies as determined by PSEUROT 6.2 analysis. The horizontal bars indicate the range of *P* values possible. Solid lines represent a summation of the Boltzmann distribution of conformers within each 5° increment at the indicated level of theory.

IV. Density Functional Theory Geometries. The gas-phase B3LYP/6-31G* distribution was superior to the gas-phase HF/6-31G* distribution in many ways (Figure 6, Table 6, compare entries 2−4). After determining the B3LYP/6-31+G** single-point energies as well as applying enthalpic and entropic corrections, the gas-phase DFT methods seemed to provide a better correlation to the solution Boltzmann distribution of **1** than the gas-phase HF methods. Most importantly, the northern and southern minimums both shifted 5−10° closer to the experimentally observed minimums upon optimization at the B3LYP/6-31G* level (Figure 6). The north/south ratio (91:9) still favors the northern ring conformers by too much compared to the experimental value, but the rotamer populations around the C_4-C_5 and C_3-O_3 bonds are closer to the experimental values than at the HF levels of theory (Table 6, compare entries 4 and 13).

The aqueous-phase B3LYP/6-31+G**//SM5.42/BPW91/6-31G* distribution also correlated well with experiment (Figure 6k,l, Table 6, compare entries 11−13). First, the identity of the northern and southern minimums were even closer to those observed experimentally than those obtained at the SM5.42/HF/6-31G* level of theory. The ^{O}E ring conformer family, the experimentally observed northern conformer, also contributed 2−5% to the Boltzmann distribution, compared to <1% in the gas phase. The north/south ratio (64:36) without inclusion of the ZPE, enthalpic, or entropic contributions of the solute (Figure

6k) correlated well with that observed experimentally. However, inclusion of the ZPE, enthalpic, and entropic contributions caused an even greater preference for the northern conformers (89:11). The predicted populations around the C_4-C_5 and C_3-O_3 bonds were comparable to those at the SM5.42/HF/6-31G* level of theory (Table 6).

V. Calculation of Coupling Constants. Comparison of the conformer distributions calculated at each level of theory with that obtained from PSEUROT analysis of the $^1H-^1H$ coupling constants was unsatisfying because it was impossible to determine which of the solvation methods correlated best with experiment (Figure 6e−h,k,l). The DFT northern and southern minimums were closest to those determined by PSEUROT; however, the HF distributions contained a larger amount of the experimentally determined northern minimum, ^OE. We reasoned that this ambiguity arises from the fact that our calculations point to a multiconformer distribution, and therefore, the two-state model assumed by PSEUROT analysis is inadequate. Therefore, although the qualitative location and percentages of the northern and southern conformers predicted by PSEUROT are reasonable, these results should not be taken as quantitative. We felt it would be desirable to calculate the average $^3J_{H1,H2}$, $^3J_{H2,H3}$, and $^3J_{H3,H4}$ values for the conformer distribution at each level of theory and then compare these results *directly* to the experimentally observed coupling constants to evaluate the accuracy of each theoretical method.

Initially, Boltzmann-weighted coupling constants for each conformer distribution were calculated using three previously reported sets of Karplus equations.[9d,37] For each contributor to the conformational ensemble, the appropriate dihedral angle was extracted and the $^3J_{H,H}$ determined for that structure. This coupling constant was, in turn, weighted by the contribution of the conformer to the Boltzmann distribution. Summation of these scaled couplings resulted in the Boltzmann-weighted coupling constants (see Supporting Information for equations and additional details). The dependence of $^3J_{H1,H2}$, $^3J_{H2,H3}$, and $^3J_{H3,H4}$ on *P* for all conformers at all levels of theory is shown in Figure 7. Data for only two sets of equations are given, those developed by Cros and co-workers[9d] (open triangles) and Donders et al.[37a] (solid diamonds). The other set of equations we investigated, reported by Altona et al.,[37b] provided results very similar to those obtained with the Donders et al. equations and hence are not presented in Figure 7. The qualitative trends are similar regardless of the equation used; however, in general, significantly larger couplings are predicted by the Cros equations. In addition, agreement between the calculated and experimental coupling constants was the poorest with the Cros equations (see Supporting Information). The discrepancy between these two methods complicated our analysis since we did not know which set of equations was "correct" for our system. We therefore pursued calculation of these coupling constants directly from the conformer geometries using density functional theory methods.

For these calculations, we chose to use the deMon-NMR program,[38] which has previously been employed to calculate $^1H-^{13}C$ coupling constants in carbohydrates, providing results in good agreement with experiment.[39] To test the ability of this program to accurately predict $^3J_{H,H}$ in carbohydrates, we carried out a series of calculations on methyl α-D-mannopyranoside, **3** (Chart 3), a molecule that adopts a single chair conformation in solution. Glycoside **3** possesses small (1.8 Hz), medium (3.5 Hz), and large (9.5 Hz) $^3J_{H,H}$, which makes it an ideal test molecule for this purpose. Calculation of the $^3J_{H,H}$ at the PW91/

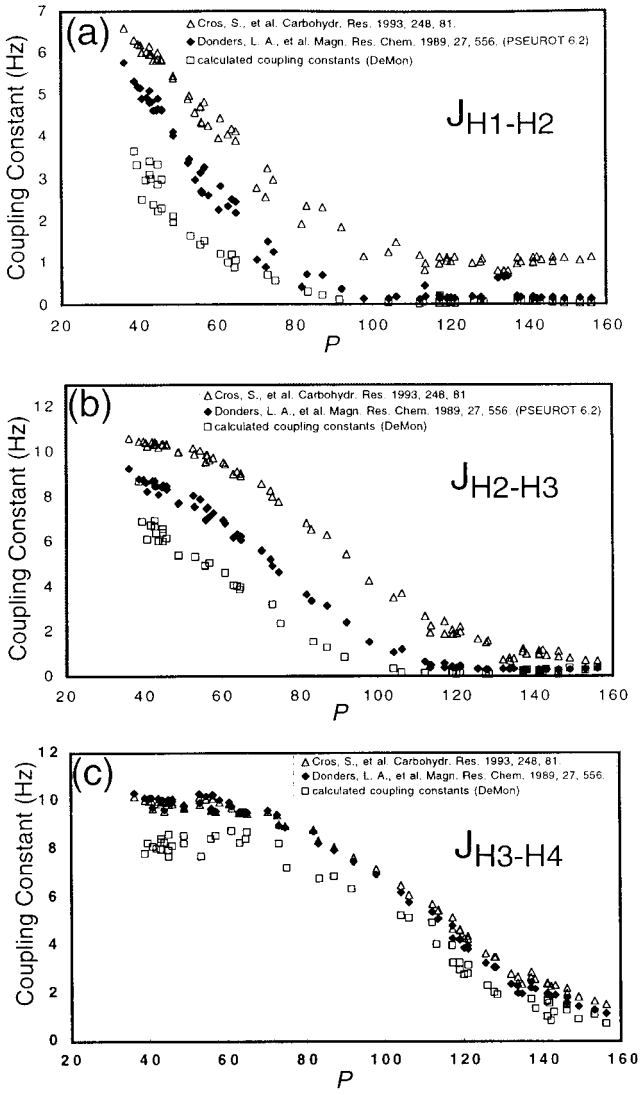

Figure 7. Relationship between *P* and $^3J_{H,H}$ for all conformers at all levels of theory. (a) $^3J_{H1,H2}$, (b) $^3J_{H2,H3}$, and (c) $^3J_{H3,H4}$ as determined with deMon and refs 9d and 37a.

Chart 3

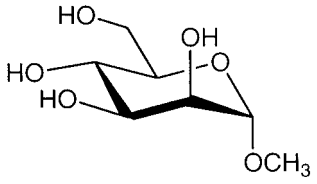

3

(37) (a) Donders, L. A.; de Leeuw, F. A. A. M.; Altona, C. *Magn. Reson. Chem.* **1989**, *27*, 556. (b) Altona, C.; Francke, R.; de Haan, R.; Ippel, J. H.; Daalmans, G. J.; Hoekzema, A. J. A. W.; van Wijk, J. *Magn. Reson. Chem.* **1994**, *32*, 670.

(38) (a) St-Amant, A.; Salahub, D. R. *Chem. Phys. Lett.* **1990**, *169*, 387. (b) Casida, M. E.; Daul, C.; Goursot, A.; Koester, A.; Pettersson, L.; Proynov, E.; St-Amant, A.; Salahub, D. R.; Duarte, H.; Godbout, N.; Guan, J.; Jamorski, C.; Leboeuf, M.; Malkin, V.; Malkina, O.; Sim, F.; Vela, A. *deMon-KS*, version 3.4; deMon Software, University of Montreal, Quebec, Canada, 1996. (c) Malkin, V. G.; Malkina, O. L.; Salahub, D. R. *Chem. Phys. Lett.* **1994**, *221*, 91. (d) Malkina, O. L.; Salahub, D. R.; Malkin, V. G. *J. Chem. Phys.* **1996**, *105*, 8793. (e) Salahub, D. R.; Fournier, R.; Mlynarski, P.; Papai, I.; St-Amant, A.; Uskio, J. In *Density Functional Methods in Chemistry*; Labanowski, J. K., Anzelm, J. W., Eds.; Springer: New York, 1991; p 77. (f) Malkin, V. G.; Malkina, O. L.; Casida, M. E.; Salahub, D. R. *J. Am. Chem. Soc.* **1994**, *116*, 5898.

(39) (a) Hricovini, M.; Malkina, O. L.; Bizik, F.; Nagy, L. T.; Malkin, V. G. *J. Phys. Chem. A* **1997**, *101*, 9756. (b) Cuevas, G.; Juaristi, E.; Vela, A. *J. Phys. Chem. A* **1999**, *103*, 932.

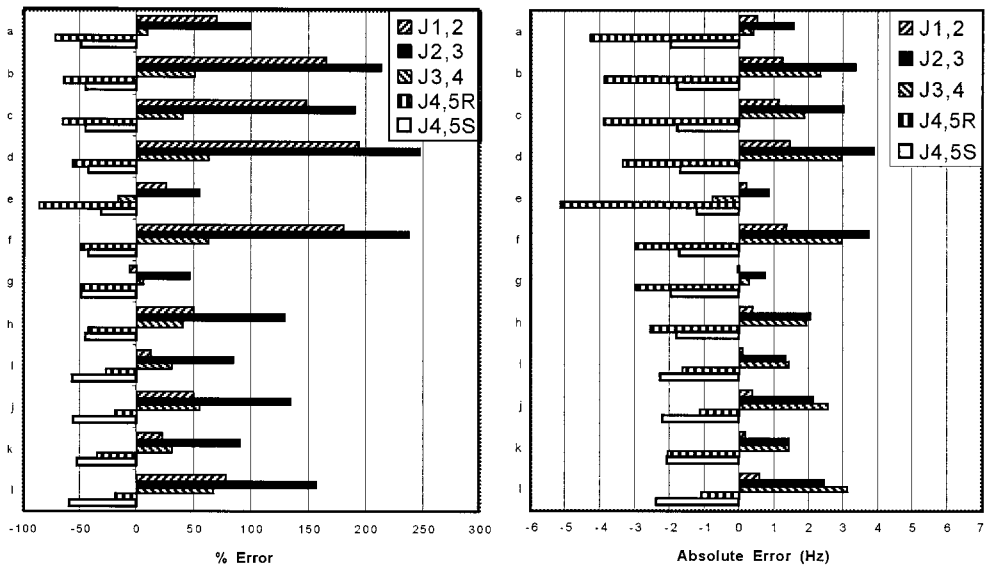

Figure 8. Difference between the Boltzmann-weighted deMon calculated $^3J_{H,H}$ at each level of theory and those measured by NMR ($^3J_{1,2} = 0.75$ Hz, $^3J_{2,3} = 1.57$ Hz, $^3J_{3,4} = 4.67$ Hz) (calculated − experimental): (a) ΔE (HF/6-31G*), (b) ΔG (HF/6-31G*), (c) ΔE (B3LYP/6-31+G**//HF/6-31G*), (d) ΔG (B3LYP/6-31+G**//HF/6-31G*), (e) ΔE (SM5.42/HF/6-31G*), (f) ΔG (SM5.42/HF/6-31G*), (g) ΔE (B3LYP/6-31+G**//SM5.42/HF/6-31G*), (h) ΔG (B3LYP/6-31+G**//SM5.42/HF/6-31G*), (i) ΔE (B3LYP/6-31+G**//B3LYP/6-31G*), (j) ΔG (B3LYP/6-31+G**//B3LYP/6-31G*), (k) ΔE (B3LYP/6-31+G**//SM5.42/BPW91/6-31G*), and (l) ΔG (B3LYP/6-31+G**//SM5.42/BPW91/6-31G*).

IGLO-III[40] level of theory for the HF/6-31G*, SM5.42/HF/6-31G*, B3LYP/6-31G*, and SM5.42/BPW91/6-31G* geometries of all three C_5-C_6 rotamers of methyl α-D-mannopyranoside gave encouraging results (see the Supporting Information for details). The deMon calculated coupling constants for the ring protons were within 20% of those measured experimentally and qualitatively correct for the trend of $^3J_{H,H}$.[41] These results suggest that the DFT-based deMon method could be used accurately to compare computationally determined conformer distributions to experimentally determined coupling constants.

Comparison of the average coupling constants determined by deMon at each level of theory with the experimental coupling constants for **1** is shown in Figure 8. The calculated $^3J_{H4,H5}$ are uniformily too small. This was also observed when the couplings were calculated with the empirical Karplus equations and was likely a result of the sensitivity of these couplings to the C_4-C_5 rotamer populations and an apparent overestimation of the contribution of the gg rotamer to the calculated Boltzman distributions. The relationship between P and each $^3J_{H,H}$ for all conformers is depicted in Figure 7 (open squares). It is clear from the results indicated in Figures 6 and 8 that the levels of theory which include the effects of solvation are more accurate than the gas-phase methods when compared to experiment. Furthermore, the best comparison is at the SM5.42/HF/6-31G* level of theory without explicit inclusion of the enthalpic and entropic contributions to the free energy (Figure 8e). When these effects are explicitly included, agreement between the NMR and calculated coupling constants of the ring protons is worse (compare Figure 8e with f). We suspect that some "double counting" of entropic effects in the Gibbs free energy may occur because of the manner in which this solvation model was initially parametrized with respect to the experimental data for free energies of solution. Analysis of Figure 7 suggests that the ring coupling constants predicted from our computational study are likely too large because the northern conformer distribution is too far to the north. This is in agreement with the data presented in Figure 6 and could possibly be remedied by the explicit inclusion of solvent molecules for some intimate solvent−solute interactions. Of course, this would significantly increase the expense of the calculations. However, even without explicit solvent−solute considerations, the SM5.42 method within the MN-GSM implementation appears to yield excellent energetic and geometric results when compared to experiment.

Conclusions

This report has described the conformational preferences of methyl 3-*O*-methyl-α-D-arabinofuranoside, **1**, at several levels of theory and has compared these results to those determined experimentally by NMR studies. These are the first ab initio and DFT investigations of a furanoside in which solvation has been addressed. This study has shown the following:

1. PSEUROT analysis of NMR coupling constant data is valuable for gaining a qualitative understanding of the conformational preferences of **1** but is of limited value if quantitative results are required. Moreover, the assumption of a two-conformer model is not realistic for **1**, since many ring conformations contribute to the Boltzmann distribution at all levels of theory.

2. The systematic pseudo Monte Carlo Search protocol available in MacroModel can be used, in conjunction with the AMBER* force field, to generate a diverse family of furanoside geometries.

3. Optimization of the AMBER conformers at the HF/6-31G* level in the gas phase reduces the number of unique conformers requiring study with the more costly DFT and solvation calculations while maintaining a high degree of structural diversity.

4. Enthalpic and entropic effects are important contributors to the relative energy among conformers of **1** in the gas and solution phases.

5. Computational studies of the solution-phase conformational preferences of saccharides such as **1** are both possible and necessary for an accurate understanding of their conformational

(40) (a) Perdew, J. P.; Wang, Y. *Phys. Rev. B* **1986**, *33*, 8800. (b) Perdew, J. P. *Phys. Rev. B* **1986**, *33*, 8822. (c) Perdew, J. P. *Phys. Rev. B* **1986**, *34*, 7406.

(41) Podlasek, C. A.; Wu, J.; Stripe, W. A.; Bondo, P. B.; Serianni, A. S. *J. Am. Chem. Soc.* **1995**, *117*, 8635.

preferences. In this regard, the MN-GSM solvation model was remarkable in its utility and success in comparison to experiment. The SM5.42/HF/6-31G* level of theory was the most successful (compared to experiment) and efficient of those examined.

6. Good agreement with experiment can be obtained through the use of a diverse population of conformations in conjunction with adequate levels of theory, especially with the inclusion of solvation.

Acknowledgment. This work was funded by grants from the National Science Foundation (CHE-9875163 and CHE-9733457) and the Ohio Supercomputer Center. J.B.H. is supported as a graduate research fellow by a NIH Training Grant for Chemistry at the Biology Interface. We thank the reviewers for their many helpful suggestions. Finally, we are grateful to Christopher J. Cramer and Donald G. Truhlar for access to the MN-GSM code at the Minnesota Supercomputer Institute. We also acknowledge assistance from James Xidos for initial help in performing some of the MN-GSM calculations.

Supporting Information Available: Details outlining the attempts to isolate conformations in the $P = 135-200°$ region, the studies used to determine the best method to reduce the number of AMBER conformers requiring HF/6-31G* optimization, the preparation of **1** and [^{13}C]-**1**, the description of PSEUROT 6.2 calculations, the methods used for determining rotamer populations about the C_4-C_5 and C_3-O_3 bonds, the calculation of coupling constants using empirical Karplus equations and the deMon-NMR program, and the geometric parameters for conformers at several levels of theory. This material is available free of charge via the Internet at http://pubs.acs.org. See any current masthead page for ordering information and Web access instructions.

JA003768S